

Understanding Regularization in Batch Normalization

Ping Luo¹ Xinjiang Wang² Wenqi Shao² Zhanglin Peng²

Abstract

Batch Normalization (BN) makes output of hidden neuron had zero mean and unit variance, improving convergence and generalization when training neural networks. This work understands these phenomena theoretically. We analyze BN by using a building block of neural networks, which consists of a weight layer, a BN layer, and a nonlinear activation function. This simple network helps us understand the characteristics of BN, where the results are generalized to deep models in numerical studies. We explore BN in three aspects. First, by viewing BN as a stochastic process, an analytical form of regularization inherited in BN is derived. Second, the optimization dynamic with this regularization shows that BN enables training converged with large maximum and effective learning rates. Third, BN's generalization with regularization is explored by using random matrix theory and statistical mechanics. Both simulations and experiments support our analyses.

1. Introduction

Batch Normalization (BN) is an indispensable component in many deep neural networks such as (He et al., 2016; Huang et al., 2017). Empirical studies (Ioffe & Szegedy, 2015) discovered that BN improves convergence and generalization by enabling large learning rate and preventing overfitting when training neural networks. Understanding BN theoretically is a key question.

We explore BN in three aspects. First, we show that the batch statistics (mean and variance) of BN *impose implicit regularization in training*, which takes an explicit form that helps us understand BN's characteristics. Second, we

analyze the optimization of BN with regularization in the regime of online learning by using stochastic gradient descent (SGD). We show that BN enables training to converge with *large maximum and effective learning rates*, which are larger than a network trained without BN or trained with weight normalization (WN) (Salimans & Kingma, 2016) (WN is a counterpart of BN). Third, we investigate the generalization of BN with regularization by using random matrix theory and statistical mechanics. We show that BN reduces overfitting and generalization errors.

In empirical studies, the above analyses in a single-layer perceptron are then extended to multi-layered networks with convolutional layers. It is observed that deep networks share the same traits of regularization of BN, serving as an explanation of its good performance in deep networks. Also, a simple regularization method can be utilized to mitigate overfitting for WN as well as for BN when training with large batch.

1.1. Notations

This work denotes a scalar by using lowercase letter (*e.g.* x), and a vector using bold lowercase letter (*e.g.* \mathbf{x}). We study BN in a building block as a single-layer perceptron, which consists of a weight layer, a BN layer, and a nonlinear activation function as shown in Fig.1 (a). Its forward computation can be written as $y = g(\hat{h})$, $\hat{h} = \gamma \frac{h - \mu_B}{\sigma_B} + \beta$, and $h = \mathbf{w}^T \mathbf{x}$, where $g(\cdot)$ denotes an activation function such as ReLU¹, h and \hat{h} are the hidden values before and after normalization, \mathbf{w} and \mathbf{x} are the weight vector and network input respectively. In BN, μ_B and σ_B represent the mean and standard deviation of h . They are estimated within a batch of M samples. γ is a scale parameter and β is a shift parameter.

Despite the simplicity of the above network, it builds up the basic blocks of deep neural networks. It has been widely adopted to analyze the performance and roles of methods such as proper initialization (Krogh & Hertz, 1992; Advani & Saxe, 2017), weight decay, data augmentation (Börs, 1998), and dropout (Wager et al., 2013). Similar to (Ba et al., 2016), our analyses assume that the neurons of BN layer are independent, as the mean and variance are

Preprint. Work in progress. The first three authors contribute equally. ¹The Chinese University of Hong Kong ²SenseTime Research. Correspondence to: Ping Luo <pluo.lhi@gmail.com>, Xinjiang Wang <wangxinjiang@sensetime.com>, Wenqi Shao <shaowenqi@sensetime.com>, Zhanglin Peng <pengzhanglin@sensetime.com>.

¹ReLU is defined as $\max(0, x)$.

Table 1. Several frequently-presented notations are summarized.

μ_B, σ_B^2	batch mean, batch variance
μ_P, σ_P^2	population mean, population variance
\mathbf{x}, \mathbf{y}	input of a network, output of a network
\bar{y}	ground truth of an output
h, \hat{h}	hidden value before and after BN
\hat{h}	hidden value after population normalization
γ, β	scale parameter, shift parameter
$g(\cdot)$	activation function
\mathbf{w}, \mathbf{w}^*	weight vector, ground truth weight vector
$\tilde{\mathbf{w}}$	normalized weight vector
M, N, P	batch size, number of neurons, sample size
α	an effective load value $\alpha = P/N$
ζ	regularization strength (coefficient)
ρ	Kurtosis of a distribution
δ	gradient of the activation function
$\eta_{\text{eff}}, \eta_{\text{max}}$	effective, maximum learning rate
R	overlapping ratio (angle) between $\tilde{\mathbf{w}}$ and \mathbf{w}^*
L	norm (length) of \mathbf{w}
$\lambda_{\text{max}}, \lambda_{\text{min}}$	maximum, minimum eigenvalue
ϵ_{gen}	generalization error

estimated individually for each neuron. But we get rid of the Gaussian assumptions on the input data and the weight vectors in theorem 1, which is our main result, meaning our assumptions are milder than those in (Salimans & Kingma, 2016; Yoshida et al., 2017).

Overall, several frequently-used notations in this work are summarized in Table 1 for reference.

1.2. Overview of Results

The results of this work are highlighted in three aspects.

(1) The regularization of BN is derived in theorem 1, showing that the stochastic behaviors of the batch estimations of μ_B and σ_B both impose l_2 regularization on the scale parameter γ , while they have different strengths and impacts in training.

- The regularization induced by μ_B *discourages* the reliance on a single neuron and *encourages* different neurons to have equal magnitude, in the sense that corrupting individual unit does not harm generalization. This is consistent with the empirical result found in (Morcos et al., 2018). The regularization of σ_B penalizes the kurtosis of distribution of input neurons as well as the entries of the Fisher Information Matrix with respect to the γ parameter. This is not found by previous empirical studies.
- Both the above regularization strengths are *inversely proportional* to the batch size M , indicating that training with large batch decreases regularization.
- The mean and variance jointly regularize training. Removing either one of them could impeded convergence

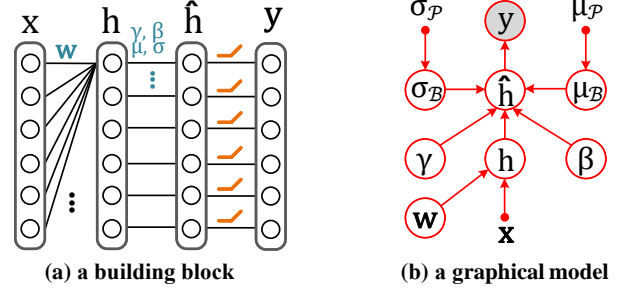


Figure 1. (a) shows the diagram of a building block with BN as a single-layer perceptron, consisting of an input layer \mathbf{x} , a hidden layer \mathbf{h} , a BN layer $\hat{\mathbf{h}}$, and an output layer \mathbf{y} with a nonlinear activation function. (b) illustrates a graphical model of the single-layer network.

and generalization. Empirical studies in real data demonstrate the above findings.

(2) With the regularization expression, we explore the learning dynamics of SGD with BN by using ordinary differential equations. We show in Sec.3 that BN enables the network converged with large maximum and effective learning rates, leading to faster training speed compared to a network trained without BN or trained with WN. The magnitude of the learning rates depend on the regularization strength.

(3) The generalization capacity of BN with regularization is analyzed under the framework of random matrix theory and statistical mechanics in Sec.4. We mainly investigate the “large-scale” regime, where the number of samples P and the number of neurons N are both large, but their ratio $\alpha = P/N$ is finite. We find that BN reduces over-training especially when $\alpha = 1$ (P and N are comparable), compared to a network trained without BN. The regularization strength of BN is quantified by both analytical and empirical studies. Numerical results support our analyses by training a convolutional neural network with multiple hidden layers on both simulated and real data.

2. A Statistical Interpretation of BN

Overview. To show the regularization of BN, we treat μ_B and σ_B as random variables in training, which are estimated by using a batch of samples. As one sample is seen many times in the entire training course and it is presented with other samples in a batch that is randomly drawn at every time, μ_B and σ_B are injected random noise for this sample. Within a probabilistic framework such as (Andersen, 1970; Ravanbakhsh et al., 2016), the single-layer perceptron in Fig.1(a) can be interpreted as a graphical model as shown in Fig.1(b), where μ_B and σ_B are random variables whose distributions are characterized by the population mean and

population standard deviation, denoted as μ_P and σ_P . The \mathbf{x} and y denote the input and the target value, h and \hat{h} are hidden variables, γ and β are the scale and shift parameter respectively, and \mathbf{w} represents the weight parameters.

Loss Function. The Gaussian distribution is often employed as prior distribution for the weight parameters, leading to l_2 regularization over \mathbf{w} . This regularization is referred as weight decay (Krizhevsky et al., 2012), which is a popular technique in deep learning. Training a neural network typically involves minimization of the negative log likelihood function with respect to a set of parameters $\theta = \{\mathbf{w}, \gamma, \beta\}$. Therefore, the loss function is defined as

$$\frac{1}{P} \sum_{j=1}^P \ell(\hat{h}^j) = -\frac{1}{P} \sum_{j=1}^P \log p(y^j | \hat{h}^j; \theta) + \zeta \|\mathbf{w}\|_2^2, \quad (1)$$

where $p(y^j | \hat{h}^j; \theta)$ is the likelihood function defined by the network, P is the number of training samples, and ζ is a coefficient of the regularization (such as weight decay).

Prior. Similar to (Teye et al., 2018), we find that BN also induces Gaussian priors for μ_B and σ_B . We have

$$\mu_B \sim \mathcal{N}(\mu_P, \frac{\sigma_P^2}{M}) \text{ and } \sigma_B \sim \mathcal{N}(\sigma_P, \frac{\rho+2}{4M}), \quad (2)$$

where M is the batch size and ρ is the Kurtosis statistic that measures the peakedness of a distribution. We have $\rho = \frac{C - \sigma_P^4}{\sigma_P^4} - 2$ and $C = \mathbb{E}[(\mathbf{w}^T \mathbf{x} - \mu_P)^4]$. A distribution with positive kurtosis is more peaked than a Gaussian distribution (*i.e.* with a heavier tail), while a distribution with negative kurtosis looks like a loaf of bread. Eqn.(2) has two intuitive meanings. First, μ_B and σ_B would induce Gaussian noise in training. When M increases, the batch statistics μ_B and σ_B would approximate the population statistics μ_P and σ_P . As the sample mean converges in probability to the population mean by the weak Law of Large Numbers, $M > 30$ would produce a good approximation. This has been also found by empirical experiment (Li et al., 2016) where batch size is 32. Second, σ_B may induce kurtosis noise produced by the batch estimation.

2.1. Regularization in BN

With Eqn.(2), the loss function in Eqn.(1) can be written as an expected loss by integrating over μ_B and σ_B , that is, $\frac{1}{P} \sum_{j=1}^P \mathbb{E}_{\mu_B, \sigma_B} [\ell(\hat{h}^j)]$, where $\mathbb{E}[\cdot]$ denotes expectation. By analyzing this expected loss function, we show that μ_B and σ_B impose l_2 regularization on the scale parameter γ , but they result in different strengths of regularization. In theorem 1, we employ ReLU activation function as a concrete example, which is widely explored in practice. In general, we show how to extend the results to the other activation functions in section 1 of Appendix.

Theorem 1 (Regularization of μ_B, σ_B). *Let ζ be the strength (coefficient) of the regularization and the activation function be ReLU. Then*

$$\frac{1}{P} \sum_{j=1}^P \mathbb{E}_{\mu_B, \sigma_B} \ell(\hat{h}^j) \simeq \frac{1}{P} \sum_{j=1}^P \ell(\bar{h}^j) + \zeta \gamma^2, \quad (3)$$

$$\text{and } \zeta = \underbrace{\frac{\rho+2}{8M} F_\gamma}_{\text{from } \sigma_B} + \underbrace{\frac{1}{2M} \frac{1}{P} \sum_{j=1}^P \sigma(\bar{h}^j)}_{\text{from } \mu_B}, \quad (4)$$

where $\bar{h}^j = \gamma \frac{\mathbf{w}^T \mathbf{x}^j - \mu_P}{\sigma_P} + \beta$, ρ is the kurtosis of the distribution of $\mathbf{w}^T \mathbf{x}$, F_γ represents the entries of Fisher Information Matrix with respect to γ , and $\sigma(\cdot)$ is a sigmoid function.

Theorem 1 tells us that the batch statistics in BN could be represented by using the population statistics with a regularization of $\zeta \gamma^2$, where ζ is the regularization strength that has two terms produced by σ_B and μ_B individually. It is derived by performing Taylor expansion of the expected loss function at $\bar{h}^j = \gamma \frac{\mathbf{w}^T \mathbf{x}^j - \mu_P}{\sigma_P} + \beta$, where the high-order terms are carefully reduced. More precisely, theorem 1 derives the analytical forms of the batch statistics in BN, where its implicit regularization is represented explicitly in ζ , enabling established methodologies such as dynamical equations and random matrix theory to be applied to understand its characteristics. Before that, we explain theorem 1 in more details.

First, the definition of \bar{h}^j in Eqn.(3) reveals a close connection between BN and WN. By following (Salimans & Kingma, 2016), WN is defined as $v \frac{\mathbf{w}^T \mathbf{x}}{\|\mathbf{w}\|_2}$, which normalizes the weight vector to have unit variance, where v is a learnable parameter. We disclose that \bar{h}^j has the form of WN when \mathbf{x} follows a Gaussian distribution with a diagonal covariance matrix. To see this, suppose that each diagonal element of the covariance matrix of \mathbf{x} is a and all the off-diagonal elements are zeros, \bar{h}^j can be rewritten as

$$\bar{h}^j = \gamma \frac{\mathbf{w}^T \mathbf{x}^j - \mu_P}{\sigma_P} + \beta = v \frac{\mathbf{w}^T \mathbf{x}^j}{\|\mathbf{w}\|_2} + b, \quad (5)$$

where $v = \frac{\gamma}{a}$ and $b = -\frac{\gamma \mu_P}{a \|\mathbf{w}\|_2} + \beta$. This equation is similar to WN with an additional bias b . Eqn.(5) imposes constraint on \mathbf{x} that might not be satisfied generally in practice. But it facilitates our understandings of the maximum and the effective learning rates depended on ζ , which is derived without using this constraint.

Second, Eqn.(4) shows that the regularization strength ζ is *inversely proportional* to the batch size M . For instance, when M increases, the regularization strength ζ decreases.

Third, Eqn.(4) shows that σ_B and μ_B produce two different regularization strengths. For example, σ_B provides a penalty depended on the Fisher Information Matrix of γ and the kurtosis ρ . And μ_B penalizes the expectation of $\sigma(\bar{h}^j)$, which represents the expected output value of a hidden neuron, implying that *the neuron with larger output may exposure to larger regularization*. Therefore, the regularization induced by μ_B encourages different neurons to have equal magnitude and discourages the reliance on a single neuron. This is consistent with the empirical results of (Morcos et al., 2018), which found that preventing the reliance of single neuron improves generalization.

3. Optimization with Regularization

Overview. This section investigates the learning dynamics of BN with regularization in a teacher-student model. We show that the model trained with BN converges with large maximum and effective learning rates, which are larger than a network trained without BN or with WN alone. Our results are consistent with the empirical studies in previous work (Ioffe & Szegedy, 2015). To our knowledge, the analyses of the maximum and the effective learning rates for BN are presented for the first time.

Our analyses are conducted in three stages. Firstly, we establish dynamical equations of the model in the thermodynamic limit and acquire the fixed point. Secondly, we investigate the eigenvalues of the Jacobian matrix at this fixed point. Finally, we perform linear stability analysis to find the maximum and the effective learning rates.

In the following we introduce useful techniques stemmed from statistical mechanics (SM) to derive the dynamical equations.

Teacher-Student Model. In SM, a student network is dedicated to learn the relationship between an input and an output with a weight vector \mathbf{w} as parameters. It is useful to characterize the learning behavior of the student by using a teacher network, which has a vector \mathbf{w}^* as a ground-truth weight vector. Here we treat a single-layer perceptron with BN as the student network, which is optimized by minimizing the l_2 distance between its output and the supervision provided by a teacher network without BN. The student and the teacher networks have identical activation function.

Loss Function. We define a loss function of the teacher-student model as $\frac{1}{P} \sum_{j=1}^P \ell(\mathbf{x}^j) = \frac{1}{P} \sum_{j=1}^P [g(\mathbf{w}^{*\top} \mathbf{x}^j) - g(\sqrt{N} \gamma \frac{\mathbf{w}^\top \mathbf{x}^j}{\|\mathbf{w}\|_2})]^2 + \zeta \gamma^2$. The first term in the square brackets represents the supervision of the teacher network, while the second term represents the output of the student network trained to mimic the teacher. The student is defined by following Eqn.(5) where $\nu = \sqrt{N} \gamma$ and N indicates the

number of neurons. The bias term is neglected for clarity of notations. In the above loss function, BN is represented by WN with the regularization $\zeta \gamma^2$, where the expression of ζ is provided in theorem 1. As we are mainly interested to investigate the impacts of ζ , the weight decay of \mathbf{w} are not included.

Let $\theta = \{\mathbf{w}, \gamma\}$ be a set of parameters. The loss function can be minimized by using SGD and θ is updated by $\theta^{j+1} = \theta^j - \eta \frac{\partial \ell(\mathbf{x}^j)}{\partial \theta^j}$, where η denotes a learning rate. The update rules for \mathbf{w} and γ are written as

$$\mathbf{w}^{j+1} - \mathbf{w}^j = \eta \delta^j \left(\frac{\gamma^j \sqrt{N}}{\|\mathbf{w}^j\|_2} \mathbf{x}^j - \frac{\tilde{\mathbf{w}}^{j\top} \mathbf{x}^j}{\|\mathbf{w}^j\|_2^2} \mathbf{w}^j \right), \quad (6)$$

$$\gamma^{j+1} - \gamma^j = \eta \left(\frac{\delta^j \sqrt{N} \mathbf{w}^{j\top} \mathbf{x}^j}{\|\mathbf{w}^j\|_2} - \zeta \gamma^j \right), \quad (7)$$

where we use $\tilde{\mathbf{w}}$ to denote the normalized weight vector of the student, that is, $\tilde{\mathbf{w}} = \sqrt{N} \gamma \frac{\mathbf{w}}{\|\mathbf{w}\|_2}$. The δ^j represents the gradient for simplicity of notations,² that is, $\delta^j = g'(\tilde{\mathbf{w}}^{j\top} \mathbf{x}^j) [g(\mathbf{w}^{*\top} \mathbf{x}^j) - g(\tilde{\mathbf{w}}^{j\top} \mathbf{x}^j)]$.

Order Parameters. As we are interested in the ‘‘large-scale’’ regime where both N and P are large and their ratio $\alpha = P/N$ is finite, it is difficult to examine a student model with parameters in high dimensions. Therefore, we transform the weight vectors to order parameters, which fully characterize the interaction between the student and the teacher. In this case, the high-dimensional parameter vector can be reparameterized by using a vector of three dimensions including γ , R , and L .

In particular, γ measures the norm of the normalized weight vector $\tilde{\mathbf{w}}$. We have $\tilde{\mathbf{w}}^\top \tilde{\mathbf{w}} = N \gamma^2 \frac{\mathbf{w}^\top \mathbf{w}}{\|\mathbf{w}\|_2^2} = N \gamma^2$. The parameter R measures the angle (overlapping ratio) between the weight vectors of the student and the teacher. We have $R = \frac{\tilde{\mathbf{w}}^\top \mathbf{w}^*}{\|\tilde{\mathbf{w}}\| \|\mathbf{w}^*\|} = \frac{1}{N \gamma} \tilde{\mathbf{w}}^\top \mathbf{w}^*$, where the norm of the ground-truth vector is $\frac{1}{N} \mathbf{w}^{*\top} \mathbf{w}^* = 1$. Moreover, L represents the norm of the original weight vector \mathbf{w} . We define $L^2 = \frac{1}{N} \mathbf{w}^\top \mathbf{w}$. In this case, the relationship between R and L can be represented by $RL = \frac{1}{N} \mathbf{w}^\top \mathbf{w}^*$.

3.1. Learning Dynamics of Order Parameters

Now we transform the update equations in (6-7) by using the above order parameters. We define three variables γ^2 , L^2 , and RL . For example, the update rule for the variable γ^2 can be obtained by $(\gamma^2)^{j+1} - (\gamma^2)^j = \frac{1}{N} [2\eta \delta^j \tilde{\mathbf{w}}^{j\top} \mathbf{x}^j - 2\eta \zeta (\gamma^2)^j]$ directly following Eqn.(7).

We can derive the update rules for the variables L^2 and RL according to Eqn.(6). For example, by multiply-

² $g'(x)$ denotes the first derivative of $g(x)$.

ing both sides of Eqn.(6) by \mathbf{w}^* , we have $(RL)^{j+1} - (RL)^j = \frac{1}{N}(\frac{\eta^j}{L^j}\delta^j\mathbf{w}^{*\top}\mathbf{x}^j - \frac{\eta R^j}{L^j}\delta^j\tilde{\mathbf{w}}^j\mathbf{x}^j)$. Similarly, we have $(L^2)^{j+1} - (L^2)^j = \frac{1}{N}[\frac{\eta^2(\gamma^2)^j}{(L^2)^j}\delta^j\mathbf{x}^j\mathbf{x}^j - \frac{\eta^2}{N(L^2)^j}\delta^j\mathbf{x}^j(\tilde{\mathbf{w}}^j\mathbf{x}^j)^2]$.

To define the learning dynamics, we turn the above update rules into a set of differential equations. We take γ^2 as an example. Its differential equation can be defined as

$$\begin{aligned} \frac{d\gamma^2}{dt} &= \lim_{\Delta t \rightarrow 0} \frac{(\gamma^2)^{j+1} - (\gamma^2)^j}{\Delta t} \\ &= 2\eta\langle\delta\tilde{\mathbf{w}}^T\mathbf{x}\rangle_{\mathbf{x}} - 2\eta\zeta\gamma^2, \end{aligned} \quad (8)$$

where $t = \frac{j}{N}$ is a normalized sample index that can be considered as a continuous time variable. We have $\Delta t = \frac{1}{N}$ that could approach zero in the thermodynamic limit when $N \rightarrow \infty$. $\langle\cdot\rangle_{\mathbf{x}}$ denotes an average over the distribution of \mathbf{x} . The differential equations of $\frac{d\gamma^2}{dt}$ and $\frac{dL^2}{dt}$ can be defined in the same way.

We simplify the notations by representing $I_1 = \langle\delta\tilde{\mathbf{w}}^T\mathbf{x}\rangle_{\mathbf{x}}$, $I_2 = \langle\delta^2\mathbf{x}^T\mathbf{x}\rangle_{\mathbf{x}}$, and $I_3 = \langle\delta\mathbf{w}^{*\top}\mathbf{x}\rangle_{\mathbf{x}}$, which are the terms presented in $\frac{d\gamma^2}{dt}$, $\frac{dRL}{dt}$, and $\frac{dL^2}{dt}$. Finally, we have a dynamical system as below

$$\frac{d\gamma}{dt} = \eta\frac{I_1}{\gamma} - \eta\zeta\gamma, \quad (9)$$

$$\frac{dR}{dt} = \eta\frac{\gamma}{L^2}I_3 - \eta\frac{R}{L^2}I_1 - \eta^2\frac{\gamma^2 R}{2L^4}I_2, \quad (10)$$

$$\frac{dL}{dt} = \eta^2\frac{\gamma^2}{2L^3}I_2. \quad (11)$$

More results of the dynamical system are provided in section 2 of Appendix.

3.2. Fixed Point of the Dynamical System

To investigate the maximum and the effective learning rates, we derive the fixed point of the dynamical system in (9-11). As we are interested in the learning rate when training converged, the above system can be linearized at small η by neglecting the terms proportional to η^2 . The investigation in small η is rational in practice, because the learning rate is always decayed to a small magnitude in order to converge to a fixed point. After that, the solution for Eqn.(9-11) follows from setting $d\gamma/dt = dR/dt = dL/dt = 0$.

By solving the above equations, the fixed points for BN, WN, and the vanilla SGD (without BN and WN) are given in Table 2, denoted as (γ_0, R_0, L_0) , which are obtained when infinite training time and samples are presented in the thermodynamic limit. In this limit, the optima for (γ_0, R_0, L_0) would be $(1, 1, 1)$. Our main interest is the overlapping ratio R_0 between the student and the teacher, because it optimizes the direction of the weight vector. We

Table 2. Comparisons of fixed points, maximum learning rates η_{\max} of R , and effective learning rates η_{eff} of R . Three methods are compared including BN, WN, and the vanilla SGD without both of them.

	(γ_0, R_0, L_0)	$\eta_{\max}(R)$	$\eta_{\text{eff}}(R)$
BN	$(\gamma_0, 1, L_0)$	$(\frac{\partial(\gamma_0 I_3 - I_1)}{\gamma_0 \partial R} - \zeta\gamma_0) / \frac{\partial I_2}{2\partial R}$	$\frac{\eta\gamma_0}{L_0^2}$
WN	$(1, 1, L_0)$	$\frac{\partial(I_3 - I_1)}{\partial R} / \frac{\partial I_2}{2\partial R}$	$\frac{\eta}{L_0^2}$
SGD	$(1, 1, 1)$	$\frac{\partial(I_3 - I_1)}{\partial R} / \frac{\partial I_2}{2\partial R}$	η

see that R_0 for all three approaches attain the optimum ‘1’. In BN and WN, this optimal solution does not depend on L_0 because their weight vectors are normalized in training. However, for the vanilla SGD, both the direction R_0 and the norm L_0 have to be optimized. Therefore, WN and BN are easier to optimize than vanilla SGD.

In BN, the value of γ_0 depends on the chosen activation function, denoted as γ_0^{bn} . For ReLU, we have $\gamma_0^{bn} = \frac{1}{2\zeta+1}$, meaning that the norm of the normalized weight vector relies on the regularization strength ζ . In comparison, as there is no regularization in WN, we have $\gamma_0^{wn} = 1$. The γ_0^{bn} of BN would lead to larger learning rates compared to WN as discussed below.

3.3. Maximum and Effective Learning Rates

With the above fixed point, we can derive the maximum and the effective learning rates when training converged. Specifically, we analyze the eigenvalues and eigenvectors of the Jacobian matrix corresponding to the system in (9-11), which determine the asymptotic convergence behavior towards the fixed point. We are specially interested in the learning rate to approach the optimum R_0 , since it optimizes the update direction of the weight vector. We find that its learning rate only depends on the eigenvalue of R , denoted as λ_R , which has the following form in general for different approaches

$$\lambda_R = \frac{\partial I_2}{\partial R} \frac{\eta\gamma_0}{2L_0^2} (\eta_{\max} - \eta_{\text{eff}}), \quad (12)$$

where η_{\max} and η_{eff} denote the maximum and the effective learning rates. We demonstrate that $\lambda_R < 0$ if and only if $\eta_{\max} > \eta_{\text{eff}}$, such that the fixed point of R is stable (see proposition 2 in Appendix). As shown in Table 2, we compare η_{\max} and η_{eff} of different approaches, leading to two observations.

First, it is able to show that the maximum learning rate of BN, denoted as η_{\max}^{bn} , is larger than those of WN and SGD, enabling R to converge with a larger learning rate. This result from the shallow network is in line with the empirical findings in (Ioffe & Szegedy, 2015), where deep networks with BN can be trained by using large learning rates. In particular, with the ReLU activation function, we find that η_{\max}^{bn} could be larger than η_{\max}^{wn} and η_{\max}^{sgd} , that is,

$\eta_{\max}^{bn} \geq \eta_{\max}^{\{wn,sgd\}} + 2\zeta$ (see proposition 3 in Appendix).

Second, BN has an effective learning rate of $\frac{\gamma_0 \eta}{L_0^2}$, which is proportional to γ_0 . This result shows that increasing the batch size M would increase the effective learning rate, as large M reduces the regularization strength ζ and rises γ . It also tells us that the common practice of synchronizing BN across GPUs to reduce noise and improve model accuracy (Peng et al., 2017) could attribute to the increase of the effective learning rate.

4. Generalization with Regularization

This section investigates the generalization of BN with regularization. To begin with, theorem 1 is verified on a single-layer perceptron with a linear activation function. Although this linear network is simple, it is suitable and it has been widely adopted to present theoretical analyses, such as early stopping (Börs, 1998), input data augmentation (Rifai et al., 2011), and dropout (Wager et al., 2013). Our analytical results of BN’s regularization are also observed in deep nonlinear networks as presented in the numerical studies in Sec.5.

Teacher-Student Model. Similar to the analysis in Sec.3, the generalization is analyzed under a teacher-student model, which minimizes a loss function of mean squared error $\frac{1}{P} \sum_{j=1}^P (\bar{y}^j - y^j)^2$, where \bar{y} represents the teacher’s output while y is the student’s output. With this model, we compare generalization of three methods, including BN, WN with regularization, and vanilla SGD without BN and WN.

All three approaches share the same teacher network, where the output of the teacher is defined as $\bar{y} = \mathbf{w}^T \mathbf{x} + \epsilon$, where \mathbf{x} is drawn from $\mathcal{N}(0, \frac{1}{N})$ and ϵ is an unobserved Gaussian noise injected to the teacher’s output. We are interested to compare the capacities of different methods to resist this noise.

vanilla SGD. For vanilla SGD, the student is computed as $y = \mathbf{w}^T \mathbf{x}$ with \mathbf{w} being the weight vector needed to be optimized in training, where \mathbf{w} has the same dimension as \mathbf{w}^* to be a realizable learning problem. The loss function of vanilla SGD is $\frac{1}{P} \sum_{j=1}^P (\mathbf{w}^{*T} \mathbf{x}^j - \mathbf{w}^T \mathbf{x}^j)^2$, whose solution asymptotically approaches the Moore–Penrose pseudo inverse solution $\mathbf{w} = (\mathbf{x}^T \mathbf{x})^+ \mathbf{x}^T \bar{\mathbf{y}}$.

BN. Here the student is defined as $y = \gamma \frac{\mathbf{w}^T \mathbf{x} - \mu_B}{\sigma_B} + \beta$, where μ_B and σ_B are estimated in a batch of M samples. As our purpose is to compare the generalization of learning the weight vector, we freeze the bias parameter similar to the vanilla SGD by freezing $\beta = 0$ in BN. Therefore, the loss function of BN is written as $\frac{1}{P} \sum_{j=1}^P (\mathbf{w}^{*T} \mathbf{x}^j - \gamma(\mathbf{w}^T \mathbf{x}^j - \mu_B)/\sigma_B)^2$.

WN with regularization. The student is computed fol-

lowing Eqn.(5) as $y = \sqrt{N} \gamma \frac{\mathbf{w}^T \mathbf{x}}{\|\mathbf{w}\|_2} + \beta$, where BN is replaced by WN since the covariance matrix of \mathbf{x} is a diagonal matrix. Similar to BN above, we freeze $\beta = 0$. Then the loss function for WN with regularization is $\frac{1}{P} \sum_{j=1}^P (\mathbf{w}^{*T} \mathbf{x}^j - \sqrt{N} \gamma \frac{\mathbf{w}^T \mathbf{x}^j}{\|\mathbf{w}\|_2})^2 + \zeta \|\gamma\|_2^2$. The expression of ζ could be derived by applying theorem 1. With the identity activation function, ζ is simplified as

$$\zeta = \lambda \left(1 + \frac{M\Gamma((M-3)/2)}{2\Gamma((M-1)/2)} - \sqrt{2M} \frac{\Gamma((M-2)/2)}{\Gamma((M-1)/2)} \right), \quad (13)$$

where λ indicates an eigenvalue of the correlation matrix of \mathbf{x} , M is the batch size, and $\Gamma(\cdot)$ is the gamma function (See the proof in Appendix).

With the above definitions, the regularization strengths of the three approaches are studied under the same learning setting. Therefore, their generalization errors can be strictly compared with the other factors ruled out. We present analytical solutions below.

4.1. Generalization Errors

Here we provide the closed-form solutions for the generalization errors of vanilla SGD and WN with regularization. They are compared with the numerical solution of BN. The generalization error is defined as the difference between error on the training set and error on the joint probability distribution of $p(\mathbf{x}, y)$. In numerical study, it is evaluated by the difference between validation loss and training loss.

vanilla SGD. The solution of weight vector depends on the rank of the correlation matrix $\Sigma = \mathbf{x}^T \mathbf{x}$. Here we define an effective load α as the ratio between the number of samples P and the number of input neurons N (the number of learnable parameters \mathbf{w}). We have $\alpha = P/N$. Then the solution is underdetermined when the effective load $\alpha < 1$, and it becomes overdetermined when $\alpha > 1$. The solution becomes unstable under noisy perturbation ϵ when $\alpha = 1$, and the generalization error diverges. Using the random matrix theory, the generalization error ϵ_{gen} can be acquired using the distribution of eigenvalues of Σ (Advani & Saxe, 2017),

$$\epsilon_{\text{gen}} = \begin{cases} 1 - \alpha + \alpha\epsilon^2/(1 - \alpha), & (\alpha < 1) \\ \epsilon^2/(1 - \alpha), & (\alpha > 1) \end{cases} \quad (14)$$

where ϵ is the injected noise to the teacher’s output. The generalization errors of vanilla SGD with respect to different values of α are plotted in the blue curve of Fig.2. It is seen that ϵ_{gen} would first decrease but then increase as α increases from 0 to 1, ϵ_{gen} diverges at $\alpha = 1$, and it would decrease again when $\alpha > 1$.

WN with regularization. The regularization term turns the correlation matrix to $\Sigma = (\mathbf{x}^T \mathbf{x} + \zeta \mathbf{I})$, which is positive

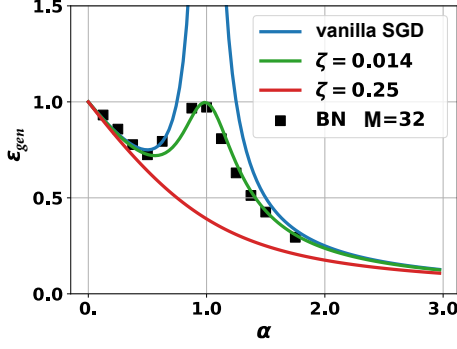


Figure 2. Comparisons of the generalization error (ϵ_{gen}) with the effective load α of vanilla SGD, WN with regularization, and BN. There are two cases of WN with regularization where $\zeta = 0.014$ and 0.25 respectively.

definite. With statistical mechanics (Krogh & Hertz, 1992), the generalization error can be derived as

$$\epsilon_{\text{gen}} = \delta^2 \frac{\partial (\zeta G)}{\partial \zeta} - \zeta^2 \frac{\partial G}{\partial \zeta}, \quad (15)$$

where G has the following formulation,

$$G = \frac{1 - \alpha - \zeta + \sqrt{(\zeta + (1 + \sqrt{\alpha})^2)(\zeta + (1 - \sqrt{\alpha})^2)}}{2\zeta}. \quad (16)$$

The expression of ζ in Eqn.(16) is derived and provided in Eqn.(13), where the eigenvalue λ of the covariance matrix Σ lies in $[\lambda^{\min}, \lambda^{\max}]$, with $\lambda^{\min} = (\sqrt{\alpha} - 1)^2$ and $\lambda^{\max} = (\sqrt{\alpha} + 1)^2$. They denote the minimum and maximum eigenvalues of Σ respectively. In this regard, ϵ_{gen} of WN with regularization can be computed quantitatively given ζ and ϵ . Let the noise variance ϵ of the teacher be 0.25. The generalization error curves with respect to α are displayed in Fig.2. We see that no other curves could outperform the curve when $\zeta = 0.25$, a value equal to the noise variance magnitude. The regularization coefficients smaller than 0.25 would exhibit over-training around $\alpha = 1$, but they perform significantly better than the vanilla SGD.

Numerical Solutions of BN. With the BN model defined above, we employ SGD with batch size $M = 32$ to find the numerical solutions of \mathbf{w} given different values of α . The total number of input features is fixed at 4096, and the number of input data points varies to change α . The generalization errors are marked as black squares in Fig.2. It is seen that the numerical results of BN clearly match the analytical curve of $\zeta = 0.014$. Given α and batch size $M = 32$, it can be figured out from Eqn.(13) that the equivalent $\zeta \approx 0.02\lambda$ where $\lambda \in [0, 4]$. The best fitter $\zeta = 0.014$ in Fig.2 lies in the range and thus quantitatively validates the derivation.

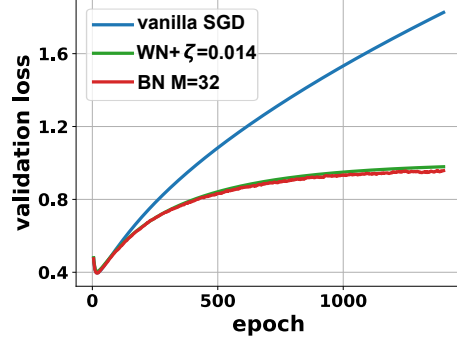


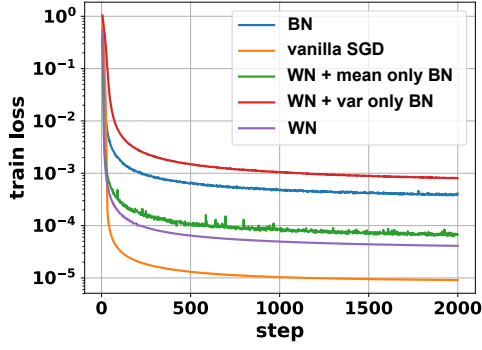
Figure 3. Comparisons of the validation loss with respect to training epochs at $\alpha = 1$, including vanilla SGD, BN, and WN with regularization.

The regularization emerged in BN is further demonstrated in the validation curve in Fig.3 for $\alpha = 1$. The curve for vanilla SGD clearly diverges while the validation error is regularized similarly for both BN at batch size $M = 32$ and WN with regularization at $\zeta = 0.014$.

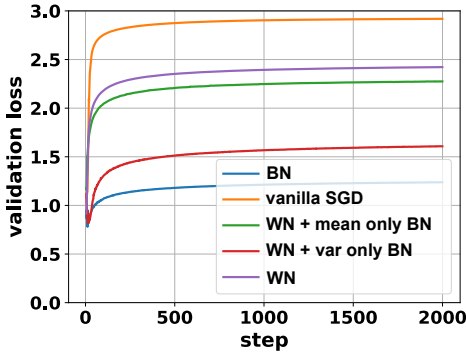
5. Empirical Studies in Convolutional Neural Networks

Setting. Here we show that our analyses can be observed in convolutional neural networks (CNNs) with multiple hidden layers. A CNN architecture similar to (Salimans & Kingma, 2016) is adopted and summarized as ‘conv(3,32)-conv(3,32)-conv(3,64)-conv(3,64)-pool(2,2)-fc(512)-fc(10)’, where ‘conv(3,32)’ represents a convolution with kernel size 3 and 32 channels, ‘pool(2,2)’ is max-pooling with kernel size 2 and stride 2, and ‘fc’ indicates a full connection. This CNN is trained on CIFAR-10 (Krizhevsky, 2009), which contains 60k natural images of 10 categories, where 50k images are used for training and the remaining images for test. We follow a configuration for training by using SGD with a momentum value of 0.9 and continuously decaying the learning rate by a factor of 10^{-4} each step. For different batch sizes, the initial learning rate is scaled proportionally with the batch size to maintain a similar learning dynamics (Goyal et al., 2017).

Comparisons of Regularization. We compare the generalization of different approaches, including vanilla SGD, BN, WN, WN with mean-only BN, and WN with variance-only BN. To diagnose the regularization strengths of different methods, the networks were all trained without any other regularization tricks such as weight decay and data augmentation. Fig.4(a) and 4(b) show the training and validation dynamics of the networks. It is found that the generalization error (*i.e.* ‘validation loss’ – ‘training loss’) using BN is much lower than that using WN and vanilla SGD. The reason behind this result has been stated in this



(a) Comparisons of training loss.



(b) Comparisons of validation loss.

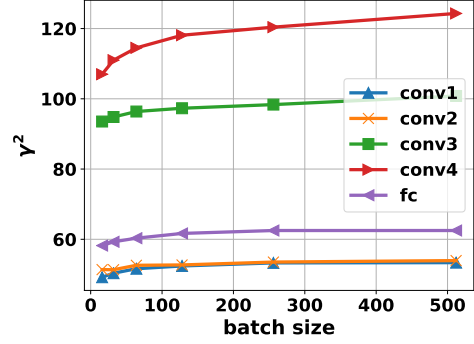
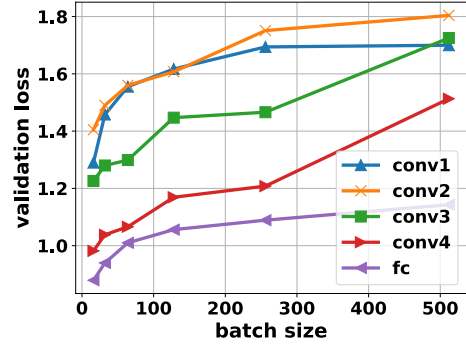
Figure 4. Training (a) and validation (b) dynamics with respect to training steps.

study, that is, BN brings in regularization ability resulting from the stochastic behaviors of μ_B and σ_B .

To investigate the regularization brought by μ_B and σ_B individually, we decompose the contribution from these two terms by running a WN with mean-only BN as well as a WN with variance-only BN, to simulate their respective regularization strengths. Compared to WN as shown in Fig.4(b), the improvements of the generalization of both mean- and variance-only BN verify the conclusion that the noises coming from μ_B and σ_B have introduced regularization of different strengths. The combination of them in BN produces the best result.

5.1. Impacts of BN

Values of γ . As shown above, the reduction of generalization errors using BN's statistics verifies Eqn.(17), where BN is decomposed into WN and regularization on γ . Here we demonstrate the impact of BN to the γ parameter. As deep models are known to suffer from multiple local minima, in order to investigate the γ value in convolutional layer, the network is first trained by using BN and relaxed to a local minima where parameters do not change much. At this local minima, the weight vector is frozen and denoted as \mathbf{w}^{bn} . Then this network is finetuned by using vanilla SGD


 (a) Relationship between γ^2 and M .


(b) Validation loss with batch size.

 Figure 5. (a) shows the relationship between batch size M and the γ values. (b) plots the change of validation loss with different batch size M .

with a small learning rate (10^{-3} in this study), where the kernel parameters are initialized as $\mathbf{w}^{sgd} = \gamma \frac{\mathbf{w}^{bn}}{\sigma}$ and σ is the moving average of σ_B .

As the stochastic behaviors of μ_B and σ_B are removed in finetuning using vanilla SGD, it is found from the last two figures of Fig.6 that the training loss decreases while the validation loss increases, meaning that the reduction in regularization makes the network converged to a sharper local minimum that generalizes less well. The magnitude of the kernel parameters \mathbf{w}^{sgd} at different layers are also displayed in the first four figures of Fig.6 and all of them increase as well when freezing BN, due to the release of regularization on these parameters.

Batch size. Moreover, in order to observe the effect of BN with different batch sizes, we evaluate BN in different layers of a network respectively. Therefore, we train five models but only add BN in one layer at a time. The regularization strength on the parameter γ is compared in Fig.5(a). The magnitude of γ increases with the increase of batch size, due to a weaker regularization for larger batches. As shown in Fig.5(b), the validation loss increases when the batch size increases, as the regularization reduces at large batch size.

BN with dropout. Despite the better generalization of the

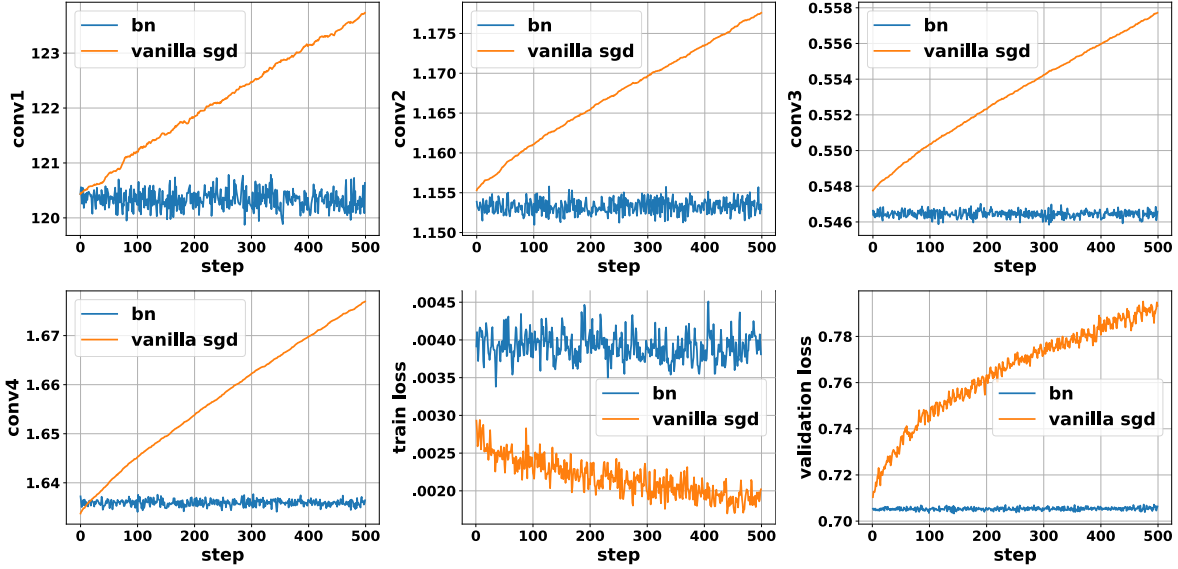


Figure 6. Finetuning results using vanilla SGD, which is finetuned from the converged network trained with BN. The first four figures show the magnitude of the kernel parameters in different layers during finetuning, compared to the results of BN. The last two figures compare the training and validation losses.

BN networks with smaller batch sizes, large-batch training is more efficient in real cases. Therefore, an effective method to improve the generalization ability of BN with large batch size is more desiring. However, it has been found that a simple decay over the γ value hardly improves the generalization for large batch sizes. A closer look at Eqn.(4) reveals that BN induces an input-data-dependent regularization coefficient ζ , which is difficult to account for in deep networks. Therefore, we utilize dropout as an alternative to compensate for the insufficient regularization. Dropout has also been analytically viewed as an adaptive regularization dependent on the input (Wager et al., 2013) and share a similar expression with Eqn.(3). Therefore, an additional dropout is added after each BN layer to impose regularization terms on γ .

Fig.7(a) and 7(b) report the results. Due to the absence of other regularization methods including data augmentation and weight decay, the generalization ability deteriorates significantly when batch size increases from 64 to 256, as is observed by the much higher validation loss and lower top-1 accuracy for $M = 256$. If a dropout layer with dropout ratio 0.125 is added *after* each BN layer for the case $M = 256$, the validation loss is suppressed and top-1 accuracy increased by a great margin. This superficially contradicts with the original claim that BN reduces the need for dropout (Ioffe & Szegedy, 2015).

There are two differences between our study and previous work (Ioffe & Szegedy, 2015). First, in pervious study the batch size was fixed at a quite small value (e.g. 32) at which the regularization was already quite strong.

Therefore, an additional dropout could not further cause better regularization, but on the contrary increases the instability of the network and yields a lower accuracy. However, in our study, the regularization degrades for BN at large batch sizes, and thus dropout with a relatively small dropout ratio can complement. Second, usual trials put dropout before BN and cause the BN layer to have different variance estimations during training and validation. However, dropout follows BN in this study and thus the above problem can be alleviated. A similar improvement of performance by applying dropout after BN has also observed by a recent work (Li et al., 2018).

WN with dropout. Since BN can be treated as WN with regularization on γ in this study, combining WN with regularization on γ should be able to match the performance of BN according to theorem 1, and the performance of WN might also be similarly improved. WN outperforms BN in running speed as it does not require calculating statistics in each step. Moreover, it suits better in RNNs than batch normalization. Therefore, an improvement of the generalization of WN is also of great importance.

Besides the regularization of $\zeta\gamma^2$, we demonstrate that WN can also be regularized by dropout following the same strategy as BN with dropout. We applied dropout after each WN layer with dropout ratio 0.25, which in fact also induces regularization on γ . We found that the improvement on both the top-1 validation accuracy and validation loss is surprising. As shown in Fig.7(b), the top-1 accuracy increases from only 0.73 to 0.80, which surpasses that of ‘BN $M = 256$ ’ and is on par with ‘BN $M = 64$ ’.

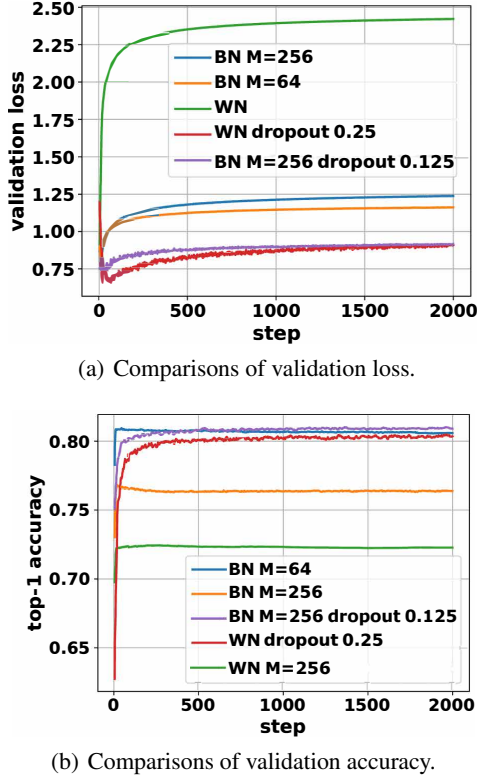


Figure 7. (a) compares the validation loss of the BN and WN networks before and after adding dropout. (b) shows the top-1 accuracy of the BN and WN networks before and after adding dropout.

6. Related Work

Neural Network Analysis. Many studies performed theoretical analyses of neural networks. For example, for a multi-layer network with linear activation function, Glorot & Bengio (2010) explored its SGD learning dynamics and Kawaguchi (2016) showed that every local minimum is global. For a nonlinear network, there are a few work such as (Oppen et al., 1990; Saad & Solla, 1996; Bs & Oppen, 1998; Pennington & Bahri, 2017; Zhang et al., 2017b; Brutzkus & Globerson, 2017; Raghu et al., 2017; Mei et al., 2016; Tian, 2017).

For instance, Tian (2017) studied the critical points and convergence behaviors of a 2-layered network with ReLU hidden units. Zhang et al. (2017b) investigated a similar teacher-student model when the activation function is harmonic. In (Saad & Solla, 1996), the learning dynamics of a committee machine were discussed when the activation function is the error function $\text{erf}(x)$. Unlike previous work, this work analyzes regularization emerged in BN and its impact to training and generalization, which are still unseen in the literature.

Normalization. Many normalization methods have been

proposed recently. For example, BN (Ioffe & Szegedy, 2015) was introduced to stabilize the distribution of the input data of each hidden layer. Weight normalization (WN) (Salimans & Kingma, 2016) decouples the lengths of the network parameter vectors from their directions, by normalizing the parameter vectors to unit length. The dynamic of WN was studied by using a single layer network (Yoshida et al., 2017). Moreover, Li et al. (2018) diagnosed the compatibility of BN and dropout (Srivastava et al., 2014) by reducing the variance shift produced by them. van Laarhoven (2017) showed that weight decay has no regularization effect when using together with BN or WN. Ba et al. (2016) demonstrated when BN or WN is employed, back-propagating gradients through a hidden layer is scale-invariant with respect to the network parameters. Santurkar et al. (2018) gave another perspective of the role of BN during training instead of reducing the covariant shift. They argued that the induced noise in batch statistics results in a smoother optimization landscape and the Lipschitzness is strengthened in networks with BN. However, analytical results of BN on its regularization and generalization are still neglected and desirable. Our study explores the regularization, optimization, and generalization of BN in the scenario of online learning.

Regularization. Ioffe & Szegedy (2015) reported that BN implicitly regularizes training to prevent overfitting. Zhang et al. (2017a) categorized BN as an implicit regularizer from experimental results. Szegedy et al. (2015) also conjectured that in the Inception network, BN behaves similar to dropout in terms of regularizing the model to improve the generalization ability. Gitman & Ginsburg (2017) experimentally compared the training performance of BN and WN and also confirmed the better generalization of BN.

In the literature there are also implicit regularization schemes other than BN. For instance, the random noise in the input layer for data augmentation has long been discovered equivalent to a weight decay method, in the sense that the inverse of the signal-to-noise ratio acts as the decay factor (Krogh & Hertz, 1992; Rifai et al., 2011). Dropout (Srivastava et al., 2014) was also proved able to regularize training by using the generalized linear model (Wager et al., 2013).

7. Discussion and Future Work

In this work, we investigated the regularization capacity emerged in BN. The analytical form of its regularization is presented by studying the stochastic behaviors of μ_B and σ_B . The convergence and generalization of a single-layer perceptron trained with BN were derived and compared with vanilla SGD and WN, showing that BN enables training to converge with large maximum and effective learning

rates, whose values depend on the regularization strength coefficient ζ . For ReLU, η_{\max}^{bn} of BN is larger than η_{\max}^{um} and η_{\max}^{sgd} by 2ζ . We also show that the regularization strength ζ improves generalization ability. Our analytical results explain many existing empirical findings. Our analyses were also observed in training deep convolutional networks. A combination of dropout and BN might ameliorate BN when batch size goes large. Our result encourages us to combine WN and dropout with an appropriate ratio, which would outperform BN and reduce the dependence on batch statistics.

In future work, an automatic strategy to regularize and improve large batch training with BN will be developed. An analytical form of optimization and regularization of CNN with BN is desirable in the community and would be investigated in the future.

References

- Advani, Madhu S. and Saxe, Andrew M. High-dimensional dynamics of generalization error in neural networks. *arXiv:1710.03667 [physics, q-bio, stat]*, October 2017. URL <http://arxiv.org/abs/1710.03667>. arXiv: 1710.03667.
- Andersen, Erling. Sufficiency and exponential families for discrete sample spaces. In *Journal of the American Statistical Association*, volume 65(331), pp. 1248–1255, 1970.
- Ba, Jimmy Lei, Kiros, Ryan, Jamie, and Hinton, Geoffrey E. Layer normalization. In *arXiv:1607.06450*, 2016.
- Brutzkus, Alon and Globerson, Amir. Globally optimal gradient descent for a convnet with gaussian inputs. In *ICML*, 2017.
- Bös, Siegfried. Statistical mechanics approach to early stopping and weight decay. *Physical Review E*, 58(1): 833, 1998.
- Bs, Siegfried and Oppel, Manfred. Dynamics of batch training in a perceptron. In *Journal of Physics A: Mathematical and General*, volume 31(21), pp. 4835, 1998.
- Gitman, Igor and Ginsburg, Boris. Comparison of Batch Normalization and Weight Normalization Algorithms for the Large-scale Image Classification. *arXiv:1709.08145 [cs]*, September 2017. URL <http://arxiv.org/abs/1709.08145>. arXiv: 1709.08145.
- Glorot, Xavier and Bengio, Yoshua. Understanding the difficulty of training deep feedforward neural networks. In *AISTATS*, 2010.
- Goyal, Priya, Dollár, Piotr, Girshick, Ross, Noordhuis, Pieter, Wesolowski, Lukasz, Kyrola, Aapo, Tulloch, Andrew, Jia, Yangqing, and He, Kaiming. Accurate, Large Minibatch SGD: Training ImageNet in 1 Hour. *arXiv preprint arXiv:1706.02677*, 2017.
- He, Kaiming, Zhang, Xiangyu, Ren, Shaoqing, and Sun, Jian. Deep residual learning for image recognition. In *CVPR*, 2016.
- Huang, Gao, Liu, Zhuang, van der Maaten, Laurens, and Weinberger, Kilian Q. Densely connected convolutional networks. In *CVPR*, 2017.
- Ioffe, Sergey and Szegedy, Christian. Batch normalization: Accelerating deep network training by reducing internal covariate shift. In *ICML*, 2015.
- Kawaguchi, Kenji. Deep learning without poor local minima. In *NIPS*, 2016.
- Krizhevsky, Alex. Learning multiple layers of features from tiny images. In *Technical Report*, 2009.
- Krizhevsky, Alex, Sutskever, Ilya, and Hinton, Geoffrey E. Imagenet classification with deep convolutional neural networks. In *NIPS*, 2012.
- Krogh, Anders and Hertz, John A. Generalization in a linear perceptron in the presence of noise. *Journal of Physics A: Mathematical and General*, 25(5):1135, 1992.
- Li, Xiang, Chen, Shuo, Hu, Xiaolin, and Yang, Jian. Understanding the disharmony between dropout and batch normalization by variance shift. In *arXiv:1801.05134*, 2018.
- Li, Yanghao, Wang, Naiyan, Shi, Jianping, Liu, Jiaying, and Hou, Xiaodi. Revisiting batch normalization for practical domain adaptation. In *arXiv:1603.04779*, 2016.
- Mei, Song, Bai, Yu, and Montanari, Andrea. The landscape of empirical risk for non-convex losses. In *arXiv:1607.06534*, 2016.
- Morcos, Ari S., Barrett, David G.T., Rabinowitz, Neil C., and Botvinick, Matthew. On the importance of single directions for generalization. In *ICLR*, 2018.
- Oppel, M., Kinzel, W., Kleinz, J., and Nehl, R. On the ability of the optimal perceptron to generalise. In *Journal of Physics A: Mathematical and General*, volume 23(11), pp. 581, 1990.
- Peng, Chao, Xiao, Tete, Li, Zeming, Jiang, Yuning, Zhang, Xiangyu, Jia, Kai, Yu, Gang, and Sun, Jian. Megdet: A large mini-batch object detector. In *arXiv:1711.07240*, 2017.

- Pennington, Jeffrey and Bahri, Yasaman. Geometry of neural network loss surfaces via random matrix theory. In *ICML*, 2017.
- Raghu, Maithra, Poole, Ben, Kleinberg, Jon, Ganguli, Surya, and Dickstein, Jascha Sohl. On the expressive power of deep neural networks. In *ICML*, 2017.
- Ravanbakhsh, Siamak, Poczos, Barnabas, Schneider, Jeff, Schuurmans, Dale, and Greiner, Russell. Stochastic neural networks with monotonic activation functions. In *AISTATS*, 2016.
- Rifai, Salah, Glorot, Xavier, Bengio, Yoshua, and Vincent, Pascal. Adding noise to the input of a model trained with a regularized objective. *arXiv:1104.3250 [cs]*, April 2011. URL <http://arxiv.org/abs/1104.3250>. arXiv: 1104.3250.
- Saad, David and Solla, Sara A. Dynamics of on-line gradient descent learning for multilayer neural networks. In *NIPS*, 1996.
- Salimans, Tim and Kingma, Diederik P. Weight normalization: A simple reparameterization to accelerate training of deep neural networks. In *arXiv:1602.07868*, 2016.
- Santurkar, Shibani, Tsipras, Dimitris, Ilyas, Andrew, and Madry, Aleksander. How Does Batch Normalization Help Optimization? (No, It Is Not About Internal Covariate Shift). *arXiv:1805.11604 [cs, stat]*, May 2018. URL <http://arxiv.org/abs/1805.11604>. arXiv: 1805.11604.
- Srivastava, Nitish, Hinton, Geoffrey, Krizhevsky, Alex, Sutskever, Ilya, and Salakhutdinov, Ruslan. Dropout: A simple way to prevent neural networks from overfitting. In *Journal of Machine Learning Research*, 2014.
- Szegedy, Christian, Vanhoucke, Vincent, Ioffe, Sergey, Shlens, Jonathon, and Wojna, Zbigniew. Rethinking the Inception Architecture for Computer Vision. *arXiv:1512.00567 [cs]*, December 2015. URL <http://arxiv.org/abs/1512.00567>. arXiv: 1512.00567.
- Teye, Mattias, Azizpour, Hossein, and Smith, Kevin. Bayesian uncertainty estimation for batch normalized deep networks. In *ICML*, 2018.
- Tian, Yuandong. An analytical formula of population gradient for two-layered relu network and its applications in convergence and critical point analysis. In *ICML*, 2017.
- van Laarhoven, Twan. L2 regularization versus batch and weight normalization. In *arXiv:1706.05350*, 2017.
- Wager, Stefan, Wang, Sida, and Liang, Percy. Dropout Training as Adaptive Regularization. *arXiv:1307.1493 [cs, stat]*, July 2013. URL <http://arxiv.org/abs/1307.1493>. arXiv: 1307.1493.
- Yoshida, Yuki, Karakida, Ryo, Okada, Masato, and ichi Amari, Shun. Statistical mechanical analysis of online learning with weight normalization in single layer perceptron. In *Journal of the Physical Society of Japan*, 2017.
- Zhang, Chiyuan, Bengio, Samy, Hardt, Moritz, Recht, Benjamin, , and Vinyals, Oriol. Understanding deep learning requires rethinking generalization. In *ICLR*, 2017a.
- Zhang, Qiuyi, Panigrahy, Rina, and Sachdeva, Sushant. Electron-proton dynamics in deep learning. In *arXiv:1702.00458*, 2017b.

Appendix

Here we outline the proofs of the results presented in the paper.

1. Proof of Theorem 1

Theorem 1 (Regularization of $\mu_{\mathcal{B}}, \sigma_{\mathcal{B}}$). *Let ζ be the strength (coefficient) of the regularization and the activation function be ReLU. Then*

$$\begin{aligned} \frac{1}{P} \sum_{j=1}^P \mathbb{E}_{\mu_{\mathcal{B}}, \sigma_{\mathcal{B}}} \ell(\hat{h}^j) &\simeq \frac{1}{P} \sum_{j=1}^P \ell(\bar{h}^j) + \zeta \gamma^2, \\ \text{and } \zeta &= \underbrace{\frac{\rho + 2}{8M} F_{\gamma}}_{\text{from } \sigma_{\mathcal{B}}} + \underbrace{\frac{1}{2M} \frac{1}{P} \sum_{j=1}^P \sigma(\bar{h}^j)}_{\text{from } \mu_{\mathcal{B}}}, \end{aligned}$$

where $\bar{h}^j = \gamma \frac{\mathbf{w}^T \mathbf{x}^j - \mu_{\mathcal{P}}}{\sigma_{\mathcal{P}}} + \beta$, ρ is the kurtosis of the distribution of $\mathbf{w}^T \mathbf{x}$, F_{γ} is a Fisher Information Matrix of γ , and $\sigma(\cdot)$ is a sigmoid function.

Proof. Let $\hat{h}^j = \gamma \frac{\mathbf{w}^T \mathbf{x}^j - \mu_{\mathcal{B}}}{\sigma_{\mathcal{B}}} + \beta$ and $\bar{h}^j = \gamma \frac{\mathbf{w}^T \mathbf{x}^j - \mu_{\mathcal{P}}}{\sigma_{\mathcal{P}}} + \beta$. We prove theorem 1 by performing a Taylor expansion on a function $A(\hat{h}^j)$ at \bar{h}^j , where $A(\hat{h}^j)$ is a function of \hat{h}^j defined according to a particular activation function. The negative log likelihood function of the single-layer perceptron can be generally defined as $-\log p(y^j | \hat{h}^j) = A(\hat{h}^j) - y^j \hat{h}^j$, which is similar to the loss function of the generalized linear models with different activation functions.

$$\begin{aligned} \frac{1}{P} \sum_{j=1}^P \mathbb{E}_{\mu_{\mathcal{B}}, \sigma_{\mathcal{B}}} [l(\hat{h}^j)] &= \frac{1}{P} \sum_{j=1}^P \mathbb{E}_{\mu_{\mathcal{B}}, \sigma_{\mathcal{B}}} [A(\hat{h}^j) - y^j \hat{h}^j] \\ &= \frac{1}{P} \sum_{j=1}^P (A(\bar{h}^j) - y^j \bar{h}^j) + \frac{1}{P} \sum_{j=1}^P \mathbb{E}_{\mu_{\mathcal{B}}, \sigma_{\mathcal{B}}} [-y^j (\hat{h}^j - \bar{h}^j) + A(\hat{h}^j) - A(\bar{h}^j)] \\ &= \frac{1}{P} \sum_{j=1}^P l(\bar{h}^j) + \frac{1}{P} \sum_{j=1}^P \mathbb{E}_{\mu_{\mathcal{B}}, \sigma_{\mathcal{B}}} [(A'(\bar{h}^j) - y^j)(\hat{h}^j - \bar{h}^j)] \\ &\quad + \frac{1}{P} \sum_{j=1}^P \mathbb{E}_{\mu_{\mathcal{B}}, \sigma_{\mathcal{B}}} \left[\frac{A''(\bar{h}^j)}{2} (\hat{h}^j - \bar{h}^j)^2 \right] \\ &= \frac{1}{P} \sum_{j=1}^P l(\bar{h}^j) + R^f + R^q, \end{aligned}$$

where $A'(\cdot)$ and $A''(\cdot)$ denote the first and second derivatives of function $A(\cdot)$. The first and second order terms in the expansion are represented by R^f and R^q respectively. To derive the analytical forms of R^f and R^q , we take a second-order Taylor expansion of $\frac{1}{\sigma_{\mathcal{B}}}$ and $\frac{1}{\sigma_{\mathcal{P}}^2}$ around $\sigma_{\mathcal{P}}$, it suffices to have

$$\frac{1}{\sigma_{\mathcal{B}}} \approx \frac{1}{\sigma_{\mathcal{P}}} + \left(-\frac{1}{\sigma_{\mathcal{P}}^2}\right)(\sigma_{\mathcal{B}} - \sigma_{\mathcal{P}}) + \frac{1}{\sigma_{\mathcal{P}}^3}(\sigma_{\mathcal{B}} - \sigma_{\mathcal{P}})^2$$

and

$$\frac{1}{\sigma_{\mathcal{B}}^2} \approx \frac{1}{\sigma_{\mathcal{P}}^2} + \left(-\frac{2}{\sigma_{\mathcal{P}}^3}\right)(\sigma_{\mathcal{B}} - \sigma_{\mathcal{P}}) + \frac{3}{\sigma_{\mathcal{P}}^4}(\sigma_{\mathcal{B}} - \sigma_{\mathcal{P}})^2.$$

By applying the distributions of $\mu_{\mathcal{B}}$ and $\sigma_{\mathcal{B}}$ in the paper, R^f can be derived as

$$\begin{aligned}
 R^f &= \frac{1}{P} \sum_{j=1}^P \mathbb{E}_{\mu_{\mathcal{B}}, \sigma_{\mathcal{B}}} \left[(A'(\bar{h}^j) - y^j) (\hat{h}^j \bar{h}^j) \right] \\
 &= \frac{1}{P} \sum_{j=1}^P \mathbb{E}_{\mu_{\mathcal{B}}, \sigma_{\mathcal{B}}} \left[(A'(\bar{h}^j) - y^j) \left(\gamma \frac{\mathbf{w}^T \mathbf{x}^j - \mu_{\mathcal{B}}}{\sigma_{\mathcal{B}}} - \gamma \frac{\mathbf{w}^T \mathbf{x}^j - \mu_{\mathcal{P}}}{\sigma_{\mathcal{P}}} \right) \right] \\
 &= \frac{1}{P} \sum_{j=1}^P \mathbb{E}_{\mu_{\mathcal{B}}, \sigma_{\mathcal{B}}} \left[(A'(\bar{h}^j) - y^j) \left(\gamma \mathbf{w}^T \mathbf{x}^j \left(\frac{1}{\sigma_{\mathcal{B}}} - \frac{1}{\sigma_{\mathcal{P}}} \right) + \gamma \left(-\frac{\mu_{\mathcal{B}}}{\sigma_{\mathcal{B}}} + \frac{\mu_{\mathcal{P}}}{\sigma_{\mathcal{P}}} \right) \right) \right] \\
 &= \frac{1}{P} \sum_{j=1}^P \gamma (A'(\bar{h}^j) - y^j) (\mathbf{w}^T \mathbf{x}^j - \mu_{\mathcal{P}}) \mathbb{E}_{\sigma_{\mathcal{B}}} \left[\frac{1}{\sigma_{\mathcal{B}}} - \frac{1}{\sigma_{\mathcal{P}}} \right] \\
 &= \frac{1}{P} \sum_{j=1}^P \frac{\rho + 2}{4M} \gamma (A'(\bar{h}^j) - y^j) \frac{\mathbf{w}^T \mathbf{x}^j - \mu_{\mathcal{P}}}{\sigma_{\mathcal{P}}}.
 \end{aligned}$$

This R^f term can be understood as below. Let $h = \frac{\mathbf{w}^T \mathbf{x} - \mu_{\mathcal{P}}}{\sigma_{\mathcal{P}}}$ and the distribution of the population data be p_{xy} . We establish the following relationship

$$\begin{aligned}
 \mathbb{E}_{(x,y) \sim p_{xy}} \mathbb{E}_{\mu_{\mathcal{B}}, \sigma_{\mathcal{B}}} [(A'(\bar{h}) - y)h] &= \mathbb{E}_{\mu_{\mathcal{B}}, \sigma_{\mathcal{B}}} \mathbb{E}_{x \sim p_x} \mathbb{E}_{y|x \sim p_{y|x}} [(A'(\bar{h}) - y)h] \\
 &= \mathbb{E}_{\mu_{\mathcal{B}}, \sigma_{\mathcal{B}}} \mathbb{E}_{x \sim p_x} \left[(\mathbb{E}[y|x] - \mathbb{E}_{y|x \sim p_{y|x}}[y])h \right] \\
 &= 0.
 \end{aligned}$$

Since the sample mean converges in probability to the population mean by the Weak Law of Large Numbers, for all $\epsilon > 0$ and a constant number K ($\exists K > 0$ and $\forall P > K$), we have $|R^f - \mathbb{E}_{(x,y) \sim p_{xy}} \mathbb{E}_{\mu_{\mathcal{B}}, \sigma_{\mathcal{B}}} [(A'(\bar{h}) - y)h]| < \frac{\rho+2}{4M} \epsilon$. The above equation means that R^f is sufficiently small given moderately large number of data points P (the above inequality holds when $P > 30$).

On the other hand, R^g can be derived as

$$\begin{aligned}
 R^g &= \frac{1}{P} \sum_{j=1}^P \mathbb{E}_{\mu_{\mathcal{B}}, \sigma_{\mathcal{B}}} \left[\frac{A''(\bar{h}^j)}{2} (\hat{h}^j - \bar{h}^j)^2 \right] \\
 &= \frac{1}{P} \sum_{j=1}^P \frac{A''(\bar{h}^j)}{2} \mathbb{E}_{\mu_{\mathcal{B}}, \sigma_{\mathcal{B}}} \left[\left(\gamma \frac{\mathbf{w}^T \mathbf{x}^j - \mu_{\mathcal{B}}}{\sigma_{\mathcal{B}}} + \beta - \gamma \frac{\mathbf{w}^T \mathbf{x}^j - \mu_{\mathcal{P}}}{\sigma_{\mathcal{P}}} + \beta \right)^2 \right] \\
 &= \frac{1}{P} \sum_{j=1}^P \frac{A''(\bar{h}^j)}{2} \mathbb{E}_{\mu_{\mathcal{B}}, \sigma_{\mathcal{B}}} \left[(\gamma \mathbf{w}^T \mathbf{x}^j)^2 \left(\frac{1}{\sigma_{\mathcal{B}}} - \frac{1}{\sigma_{\mathcal{P}}} \right)^2 - 2\gamma \mu_{\mathcal{P}} \mathbf{w}^T \mathbf{x}^j \left(\frac{1}{\sigma_{\mathcal{B}}} - \frac{1}{\sigma_{\mathcal{P}}} \right)^2 + \left(\frac{\mu_{\mathcal{B}}}{\sigma_{\mathcal{B}}} - \frac{\mu_{\mathcal{P}}}{\sigma_{\mathcal{P}}} \right)^2 \right] \\
 &\simeq \frac{1}{P} \sum_{j=1}^P \frac{\gamma^2 A''(\bar{h}^j)}{2} \left((\mathbf{w}^T \mathbf{x}^j - \mu_{\mathcal{P}})^2 \mathbb{E}_{\mu_{\mathcal{B}}, \sigma_{\mathcal{B}}} \left[\left(\frac{1}{\sigma_{\mathcal{B}}} - \frac{1}{\sigma_{\mathcal{P}}} \right)^2 \right] + \mathbb{E}_{\mu_{\mathcal{B}}, \sigma_{\mathcal{B}}} \left[\left(\frac{\mu_{\mathcal{B}} - \mu_{\mathcal{P}}}{\sigma_{\mathcal{B}}} \right)^2 \right] \right) \\
 &= \frac{1}{P} \sum_{j=1}^P \frac{\gamma^2 A''(\bar{h}^j)}{2} \left(\left(\frac{\mathbf{w}^T \mathbf{x}^j - \mu_{\mathcal{P}}}{\sigma_{\mathcal{P}}} \right)^2 \frac{\rho + 2}{4M} + \frac{1}{M} \left(1 + \frac{3(\rho + 2)}{4M} \right) \right).
 \end{aligned}$$

Note that $\frac{\partial^2 l(\bar{h}^j)}{\partial \gamma^2} = A''(\bar{h}^j) \left(\frac{\mathbf{w}^T \mathbf{x}^j - \mu_{\mathcal{P}}}{\sigma_{\mathcal{P}}} \right)^2$, we have $F(\gamma) = \frac{1}{P} \sum_{j=1}^P A''(\bar{h}^j) \left(\frac{\mathbf{w}^T \mathbf{x}^j - \mu_{\mathcal{P}}}{\sigma_{\mathcal{P}}} \right)^2$ been an estimator of the Fisher Information Matrix (FIM) with respect to the scale parameter γ , according to the definition of Fisher information. Then, by neglecting $O(1/M^2)$ high-order term in R^g , we get

$$R^g \simeq \frac{\rho + 2}{8M} F(\gamma) \gamma^2 + \frac{\mu_{\mathcal{B}}^2}{2M} \gamma^2,$$

where $\mu_{d^2 A}$ indicates the mean of the second derivative of $A(h)$.

ReLU. For the ReLU non-linearity $f(h) = \max(h, 0)$, we use its continuous approximation softplus function $f(h) = \log(1 + \exp(h))$ to derive the partition function $A(h)$. In this case, we have $\mu_{d^2 A} = \frac{1}{P} \sum_{j=1}^P \sigma(\bar{h}^j)$. Therefore, we have $\zeta = \frac{\rho+2}{8M} F(\gamma) + \frac{1}{2M} \frac{1}{P} \sum_{j=1}^P \sigma(\bar{h}^j)$.

Linear. For a loss function in the form $L = \frac{1}{P} \sum_{j=1}^P (\mathbf{w}^{*T} \mathbf{x}^j - \gamma(\mathbf{w}^T \mathbf{x}^j)/\sigma_B)^2$, $F(\gamma) = 2\lambda$ and the regularization contribution from μ_B can be neglected. $\rho = 0$ for Gaussian input distribution. Therefore, $\zeta = \frac{\lambda}{2M}$ when $M > 32$. The exact expression of theorem 1 is also possible for such linear regression problem. Under the condition of Gaussian input $\mathbf{x} \sim \mathcal{N}(0, 1/N)$, $h = \mathbf{w}^T \mathbf{x}$ is also a random variable satisfying a normal distribution $\mathcal{N}(0, 1)$, it can be derived that $\mathbb{E}(\sigma_B^{-1}) = \frac{\sqrt{M}}{\sqrt{2}\sigma_P} \frac{\Gamma(\frac{M-2}{2})}{\Gamma(\frac{M-1}{2})}$ and $\mathbb{E}(\sigma_B^{-2}) = \frac{M}{\sigma_P^2} \frac{\Gamma(\frac{M-1}{2}-1)}{\Gamma(\frac{M-1}{2})}$, therefore

$$\zeta = \lambda \left(1 + \frac{M\Gamma((M-3)/2)}{2\Gamma((M-1)/2)} - \sqrt{2M} \frac{\Gamma((M-2)/2)}{\Gamma((M-1)/2)} \right).$$

□

2. Dynamical Equations

Here we discuss the dynamical equations of BN. Let the length of teacher's weight vector be 1, that is, $\frac{1}{N} \mathbf{w}^{*T} \mathbf{w}^* = 1$. We introduce a normalized weight vector of the student as $\tilde{\mathbf{w}} = \sqrt{N} \gamma \frac{\mathbf{w}}{\|\mathbf{w}\|}$. Then the overlapping ratio between teacher and student, the length of student's vector, and the length of student's normalized weight vector are $\frac{1}{N} \tilde{\mathbf{w}}^T \mathbf{w}^* = QR = \gamma R$, $\frac{1}{N} \tilde{\mathbf{w}}^T \tilde{\mathbf{w}} = Q^2 = \gamma^2$, and $\frac{1}{N} \mathbf{w}^T \mathbf{w} = L^2$ respectively, where $Q = \gamma$. And we have $\frac{1}{N} \mathbf{w}^T \mathbf{w}^* = LR$.

We write the dynamical equations of BN as follows,

$$\begin{cases} \frac{dQ}{dt} = \eta \frac{I_1}{Q} - \eta \zeta Q, \\ \frac{dR}{dt} = \eta \frac{Q}{L^2} I_3 - \eta \frac{R}{L^2} I_1 - \eta^2 \frac{Q^2 R}{2L^4} I_2, \\ \frac{dL}{dt} = \eta^2 \frac{Q^2}{2L^3} I_2, \end{cases}$$

where $I_1 = \langle \delta \tilde{\mathbf{w}}^T \mathbf{x} \rangle_{\mathbf{x}}$, $I_2 = \langle \delta^2 \mathbf{x}^T \mathbf{x} \rangle_{\mathbf{x}}$, and $I_3 = \langle \delta \mathbf{w}^{*T} \mathbf{x} \rangle_{\mathbf{x}}$.

Proposition 1. Let λ_Q^{bn} , λ_R^{bn} be the eigenvalues of the Jacobian matrix at $\theta_0 = (Q_0, 1, L_0)$ corresponding to the order parameters Q and R respectively in BN. Then

$$\begin{cases} \lambda_Q^{bn} = \frac{\eta}{Q_0} \frac{\partial I_1}{\partial Q} - \eta \zeta Q_0, \\ \lambda_R^{bn} = \frac{\partial I_2}{2\partial R} \frac{\eta Q_0}{2L_0^2} (\eta_{\max}^{bn} - \eta_{\text{eff}}^{bn}), \end{cases}$$

where η_{\max}^{bn} and η_{eff}^{bn} are the maximum and effective learning rates respectively in BN.

Proof. Firstly, note that the change of L will not change I_1 , I_2 and I_3 . Thus we have $\frac{\partial I_1}{\partial L} = \frac{\partial I_2}{\partial L} = \frac{\partial I_3}{\partial L} = 0$. And we also neglect the term proportional to η^2 because of the learning rate decays to a small value when converged. At fixed point $R_0 = 1$, we have $\partial(QI_3 - I_1)/\partial Q = 0$, thus the Jacobian of BN is

$$J^{bn} = \begin{bmatrix} \frac{\eta}{Q_0} \frac{\partial I_1}{\partial Q} - 2\eta \zeta & \frac{\eta}{Q_0} \frac{\partial I_1}{\partial R} & 0 \\ 0 & \frac{\eta}{L_0^2} \left(\frac{Q_0 \partial I_3}{\partial R} - \frac{\partial I_1}{\partial R} - \zeta Q_0^2 \right) - \frac{\eta^2 Q_0^2}{2L_0^4} \frac{\partial I_2}{\partial R} & 0 \\ 0 & \frac{\eta^2 Q_0^2}{2L_0^3} \frac{\partial I_2}{\partial R} & 0 \end{bmatrix},$$

and the eigenvalues of J^{bn} can be obtained by inspection

$$\begin{cases} \lambda_Q^{bn} = \frac{\eta}{Q_0} \frac{\partial I_1}{\partial Q} - 2\eta\zeta, \\ \lambda_R^{bn} = \frac{\eta}{L_0^2} \left(\frac{Q_0 \partial I_3}{\partial R} - \frac{\partial I_1}{\partial R} - \zeta Q_0^2 \right) - \frac{\eta^2 Q_0^2}{2L_0^4} \frac{\partial I_2}{\partial R} = \frac{\partial I_2}{\partial R} \frac{\eta Q_0}{2L_0^2} (\eta_{\max}^{bn} - \eta_{\text{eff}}^{bn}), \\ \lambda_L^{bn} = 0. \end{cases}$$

Since $\gamma_0 = Q_0$, we have $\eta_{\max}^{bn} = (\frac{\partial(\gamma_0 I_3 - I_1)}{\gamma_0 \partial R} - \zeta \gamma_0) / \frac{\partial I_2}{2 \partial R}$ and $\eta_{\text{eff}}^{bn} = \frac{\eta \gamma_0}{L_0^2}$. \square

Proposition 2. When activation function is ReLU or sigmoid, then (i) $\lambda_Q^{bn} < 0$, and (ii) $\lambda_R^{bn} < 0$ iff $\eta_{\max}^{bn} > \eta_{\text{eff}}^{bn}$.

Proof. Firstly, when activation function is ReLU, we derive $I_1 = \frac{Q(\pi R + 2\sqrt{1-R^2} + 2R \arcsin(R))}{4\pi} - \frac{Q^2}{2}$, which gives

$$\frac{\partial I_1}{\partial Q} = -Q + \frac{\pi R + 2\sqrt{1-R^2} + 2R \arcsin(R)}{4\pi}.$$

Therefore at the fixed point of BN $\theta_0^{bn} = (\frac{1}{2\zeta+1}, 1)$, we have

$$\lambda_Q^{bn} = \eta \left(\frac{1}{Q_0} \frac{\partial I_1}{\partial Q} - 2\zeta \right) = \eta \left(\frac{1}{Q_0} \left(-1 + \frac{1}{2Q_0} - 2\zeta \right) \right) = -\zeta - \frac{1}{2} < 0.$$

Note that $\mathbf{x}^T \mathbf{x}$ approximately equals 1. We get

$$\begin{aligned} I_2 &= \int_{u,v} [g'(s) (g(t) - g(s))]^2 Ds Dt \\ &= \int_0^{+\infty} \int_0^{+\infty} v^2 Ds Dt + \int_0^{+\infty} \int_{-\infty}^{+\infty} s^2 Ds Dv - 2 \int_0^{+\infty} \int_{-\infty}^{+\infty} st Ds Dt \\ &= \frac{Q^2}{2} + \frac{\pi R + 2R\sqrt{1-R^2} + 2 \arcsin(R)}{4\pi} - \frac{Q(\pi R + 2\sqrt{1-R^2} + 2R \arcsin(R))}{2\pi}. \end{aligned}$$

At the fixed point we have $\frac{\partial I_2}{\partial R} = -Q_0 < 0$. Therefore, we conclude that $\lambda_R^{bn} < 0$ iff $\eta_{\max}^{bn} > \eta_{\text{eff}}^{bn}$.

Secondly, when activation function is sigmoid, we employ $\text{erf}(x/\sqrt{2})$ to analyze sigmoid function. Therefore, we have

$$\begin{aligned} I_1 &= \int_{u,v} [g'(u) (g(v) - g(u) u)] Du Dv \\ &= \int_{-\infty}^{+\infty} \int_{-\infty}^{+\infty} g'(u) g(v) u Du Dv - \int_{-\infty}^{+\infty} \int_{-\infty}^{+\infty} g'(u) g(u) u Du Dv. \end{aligned}$$

By using the Fourier Transformation of integral on multivariate Gaussian probability density, that is,

$$\begin{aligned} &\int \frac{dx_1 \cdots dx_n}{\sqrt{(2\pi)^n |C|}} \exp\left\{-\frac{1}{2} X^T C^{-1} X\right\} \times f_1(x_1) \cdots f_n(x_n) \\ &= \int \frac{dy_1 \cdots dy_n}{\sqrt{(2\pi)^n}} \exp\left\{-\frac{1}{2} Y^T C Y\right\} \times \tilde{f}_1(y_1) \cdots \tilde{f}_n(y_n), \end{aligned}$$

where $\tilde{f}_j(y) = \int \frac{dx}{\sqrt{2\pi}} f_j(x) e^{iyx}$.

It suffices to have

$$I_1 = \frac{2QR}{(\pi + \pi Q^2) \sqrt{2 + 2Q^2 - Q^2 R^2}} - \frac{2Q^2}{(\pi + \pi Q^2) \sqrt{1 + 2Q^2}}$$

and

$$I_2 = \frac{4}{\pi\sqrt{1+2Q^2}} \left(\arcsin \frac{1}{1+3Q^2} - \arcsin \frac{1}{\sqrt{1+3Q^2}\sqrt{2(1+2Q^2)-2Q^2R^2}} \right).$$

At the fixed point $\theta_0^{bn} = (\frac{1}{2\zeta+1}, 1)$, it can be shown that $\frac{\partial(I_1/Q)}{\partial Q} < 0$ and thus $\lambda_Q^{bn} = \eta(\frac{\partial(I_1/Q)}{\partial Q} - \zeta) < 0$, we have $\frac{\partial I_2}{\partial R} < 0$. We also conclude that $\lambda_R^{bn} < 0$ iff $\eta_{\max}^{bn} > \eta_{\text{eff}}^{bn}$. \square

Proposition 3. *When the activation function is ReLU, then $\eta_{\max}^{bn} \geq \eta_{\max}^{\{wn,sgd\}} + 2\zeta$, where η_{\max}^{bn} and $\eta_{\max}^{\{wn,sgd\}}$ indicate the maximum learning rates of BN, WN, and vanilla SGD respectively.*

Proof. From the above results, we have $I_1 = \frac{Q(\pi R + 2\sqrt{1-R^2} + 2R \arcsin(R))}{4\pi} - \frac{Q^2}{2}$, which gives $\partial I_1 / \partial R \geq 0$ at the fixed point of BN. And we get

$$\begin{aligned} I_3 &= \int_{u,v} [g'(s)(g(t) - g(s)t)] DsDt \\ &= \int_{u,v} g'(s)g(t)t DsDt - \int_{u,v} g'(s)g(s)t DsDt \\ &= \int_0^{+\infty} \int_0^{+\infty} t^2 DsDt - \int_0^{+\infty} \int_{-\infty}^{+\infty} st DsDt \\ &= \frac{\pi + 2R\sqrt{1-R^2} + 2 \arcsin(R)}{4\pi} - \frac{QR}{2}. \end{aligned}$$

Then we derive that $\frac{\partial I_2}{\partial R} < 0$ and $\frac{\partial(I_3-I_1)}{\partial R} / \frac{\partial I_2}{\partial R}$ has the same value at their respective fixed point of BN, WN and vanilla SGD. At the fixed point of BN, $Q_0 = \gamma_0 = \frac{1}{2\zeta+1} < 1$, then we have

$$\begin{aligned} \eta_{\max}^{bn} &= \left(\frac{\partial(\gamma_0 I_3 - I_1)}{Q_0 \partial R} - \zeta \gamma_0 \right) / \frac{\partial I_2}{2\partial R} \\ &= \frac{\partial(I_3 - I_1)}{\partial R} / \frac{\partial I_2}{2\partial R} + \left(1 - \frac{1}{\gamma_0}\right) \frac{\partial I_1}{\partial R} / \frac{\partial I_2}{2\partial R} - \zeta \gamma_0 / \frac{\partial I_2}{2\partial R} \\ &\geq \frac{\partial(I_3 - I_1)}{\partial R} / \frac{\partial I_2}{2\partial R} + 2\zeta \\ &= \eta_{\max}^{\{wn,sgd\}} + 2\zeta. \end{aligned}$$

\square